JOC The Journal of Organic Chemistry

Article

pubs.acs.org/joc

Switching of the Diastereomer Deposited during the Crystallization of *N*-[(*S*)-1-Phenylethyl]-2′-carbamoyl-1,1′-binaphthalene-2-carboxylic Acid: Investigation of the Mechanism of Dielectrically Controlled Resolution

Yuichi Kitamoto,[†] Kazumi Suzuki,[†] Naoya Morohashi,[†] Kenichi Sakai,[‡] and Tetsutaro Hattori*[,†]

[†]Department of Biomolecular Engineering, Graduate School of Engineering, Tohoku University, 6-6-11 Aramaki-Aoba, Aoba-ku, Sendai 980-8579, Japan

[‡]Technology Development Division, Toray Fine Chemicals Co., Ltd., 9-1 Oe-Cho, Minato-ku, Nagoya 455-8502, Japan

Supporting Information

ABSTRACT: Dielectrically controlled resolution (DCR) has been achieved during the crystallization of (*S*)-1-phenylethylamides of racemic 1,1′-binaphthalene-2,2′-dicarboxylic acid (RS_a,S)-**1**. For example, a water well-shaped plot is obtained for the diastereomeric excess (de) of the deposited amide versus the solvent permittivity (ε) for the crystallization of (RS_a,S)-**1** from three-component mixed solvents, consisting of 25 vol % of dichloromethane and 75 vol % of varying ratios of two solvents (i.e., an alcohol and either hexane or water). The de value drastically changes within two narrow ε ranges and diastereomerically pure crystals of either (R_a,S)-**1** ($13.9 \le \varepsilon \le 17.9$) or ($S_a,S$)-**1**·$CH_2Cl_2$ ($\varepsilon \le 11.9$ and $\varepsilon \ge 21.8$) deposit, depending on the solvent permittivity. X-ray crystallographic analyses reveal that the major difference between the crystal structures of (S_a,S)-**1** and (R_a,S)-**1** is the presence of solvent molecules that fill the spatial voids in the (S_a,S)-**1** crystals. The ε-dependence of the chemical shifts of (S_a,S)-**1** and (R_a,S)-**1** suggests that their aggregation states are similar in the same solvents and change discontinuously at two ε values. The ε-dependence of the C═O stretching vibrations suggests that the lower ε is a transition point where the amide molecules, which aggregate through intermolecular hydrogen bonds in low-permittivity solvents, begin to dissociate. An absorption experiment suggests that dichloromethane is easily incorporated into solvent-free (S_a,S)-**1** crystals in high-permittivity solvents. On the basis of these observations, a feasible molecular mechanism is proposed for the present DCR phenomenon.

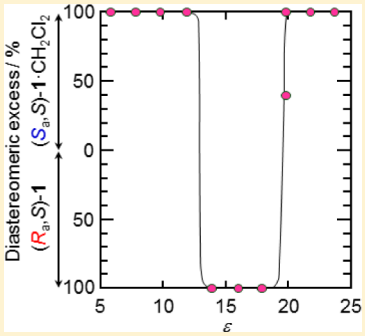

INTRODUCTION

Diastereomeric salt formation is a method used to resolve a racemic acid or base by fractional crystallization after conversion into a pair of diastereomeric salts with an enantiopure resolving agent.[1] It is one of the most important methods for enantiomeric resolution in the laboratory and industry, owing to the ease of operation, lack of special equipment required, and wide applicability. It has been estimated that this method is employed during the manufacturing of more than half of the currently marketed chiral drugs.[2] Rapid screening methods to find the most suitable resolving agent have been investigated.[3] The simultaneous use of structurally related resolving agents (Dutch Resolution) improves the crystallization rate and diastereoselectivity, as compared to the use of individual resolving agents.[4] Diastereomeric salt formation is often combined with racemization in solution, and the resulting method, which is called crystallization-induced diastereomer transformation, has been successfully applied for the preparation of chiral drugs and drug candidates.[5]

For the industrial application of diastereomeric salt formation, it is not practical to isolate the more soluble salt from the mother liquid after crystallization of its counterpart because it requires difficult and costly manipulations. Therefore, when one enantiomer of a target molecule is crystallized with the (*S*)-enantiomer of a resolving agent as the less soluble diastereomeric salt, the resolution of the antipode necessitates the (*R*)-enantiomer of the agent. This one-to-one relationship between a specific enantiomer of a resolving agent and that of a target molecule creates difficulties when the matched enantiomer of a resolving agent is unavailable. However, in 2004, Sakai, Sakurai, and co-workers proposed a novel method called dielectrically controlled resolution (DCR) that enables both enantiomers of a target molecule to precipitate as the less-soluble diastereomeric salt using a single enantiomer of a resolving agent by optimizing the permittivity of the resolving solvent for the target enantiomers.[6,7] We have a keen interest in the DCR phenomenon as it reveals that the permittivity of achiral media plays an important role in determining the selectivity of chiral discrimination; the idea has been overlooked during the long history of research on diastereomeric salt formation, for over 150 years since Pasteur resolved racemic acid with cinchona alkaloids.[8] The first observation of

Received: November 5, 2012
Published: December 10, 2012

DCR occurred during the enantiomeric resolution of α-amino-ε-caprolactam (ACL) with *N*-tosyl-(*S*)-phenylalanine [(*S*)-TPA]; (*S*)-ACL deposited selectively in the solvents with dielectric constants between 29 and 58 to give a diastereomeric salt formulated as (*S*)-ACL·(*S*)-TPA·H_2O with up to 100% de, while (*R*)-ACL deposited selectively in the solvents with either lower (5−27) or higher (62−78) ε values to give (*R*)-ACL·(*S*)-TPA with up to 69% de.[7] Since then, DCR has been successfully applied to a growing number of acid−base systems.[9−14] A common feature observed in DCR systems is that two diastereomeric salt crystals have different compositions. In most cases, one salt contains water and the other does not, as in the resolution of ACL with (*S*)-TPA; other inclusion molecules, such as ethanol[12] and 1,4-dioxane,[13] are also possible. On the basis of a close inspection of the X-ray crystal structures of the diastereomeric salts, Sakai, Hirayama, and co-workers proposed the molecular mechanism of DCR as follows:[15,16] In a low-permittivity solvent, the polar moieties of the resolving agent molecules aggregate to form a tight chiral discrimination field. As the solvent permittivity increases, the agent molecules are disaggregated by solvation, which loosens the chiral discrimination field. The DCR phenomenon is expected when the two enantiomers of a target molecule fit into the tight and loose chiral discrimination fields, respectively. The inclusion of a third component is believed to be necessary as a space filler for crystals grown in the loose chiral discrimination field in order to achieve close crystal packing. Hirose and co-workers attempted to correlate the feasibility of DCR in a resolution system with the differences in the optical rotation value and its ε-dependency between a pair of diastereomeric salts.[12,17]

In a preliminary communication,[18] we reported that the DCR phenomenon was observed during the crystallization of a 1:1 diastereomeric mixture of (*S*)-1-phenylethylamides of racemic 1,1′-binaphthalene-2,2′-dicarboxylic acid (RS_a,S)-**1**.[19] This extension of DCR to the covalent diastereomers requires reconsideration of the molecular mechanism because the resolving agent can no longer form chiral discrimination fields by itself. Our mechanistic studies suggest that a third component incorporated into one diastereomer crystal plays an active role in determining the diastereomer that deposits from high-permittivity solvents. Herein, we describe in detail the DCR phenomenon observed during the crystallization of amide (RS_a,S)-**1** and discuss its molecular mechanism.

RESULTS AND DISCUSSION

Application of DCR to the Crystallization of Amide (RS_a,S)-1. In our preliminary studies,[18] we found that the crystallization of amide (RS_a,S)-**1** gave diastereomerically pure (S_a,S)-**1** or (R_a,S)-**1** depending on the solvent employed (Scheme 1); sterically undemanding solvents, such as dichloromethane, acetone, and acetonitrile, afforded (S_a,S)-**1**·solvent crystals, whereas bulkier solvents, such as toluene and 1-propanol, afforded solvent-free (R_a,S)-**1** crystals. Accordingly, (RS_a,S)-**1** was crystallized from three-component mixed solvents, consisting of 25 vol % of a solvent that can be incorporated into the (S_a,S)-**1** crystal and 75 vol % of a mixture of two other solvents. The permittivity of the mixed solvent was varied by changing the volumetric ratio of the latter two solvents and/or replacing one of them with another solvent.[20] To induce crystallization, amide (RS_a,S)-**1** was dissolved to near saturation in each mixed solvent at 40−50 °C and then held between −1 and −2 °C for 2−3 days. Figure 1 shows the

Scheme 1. Crystallization of Amide (RS_a,S)-1 from Various Solvents

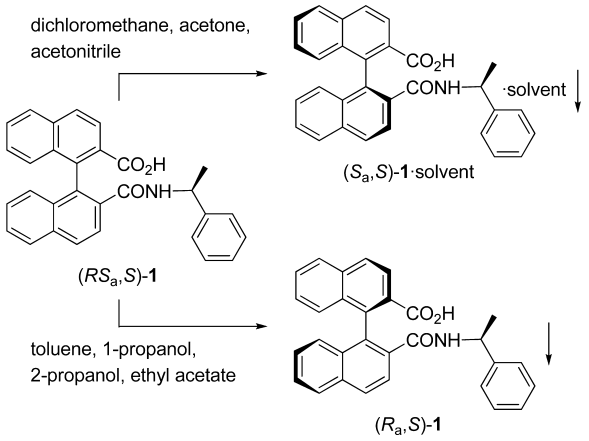

change in the diastereomeric excess of the deposited amide in different solvent systems. For the crystallization from mixtures of acetonitrile, 1-propanol, and either hexane or water, the de value drastically changed within a narrow ε range (i.e., 24.5 < ε < 29.1) and diastereomerically pure (S_a,S)-**1**·CH_3CN and (R_a,S)-**1** deposited from mixed solvents with lower and higher ε values, respectively (Figure 1a). Furthermore, (S_a,S)-**1**·CH_3CN preferentially crystallized again at a higher ε value (47.0); attempts to further increase the permittivity resulted in phase separation of the mixed solvent. When acetonitrile was replaced with dichloromethane, a similar water well-shaped change occurred in a lower and narrower ε range (12.0 < ε < 19.9) and diastereomerically pure (S_a,S)-**1**·CH_2Cl_2 deposited at both lower and higher ε values (Figure 1b). In contrast, (S_a,S)-**1**·CH_3COCH_3 precipitated from mixtures of acetone, 1-propanol, and either hexane or water in only a low ε range (Figure 1c). This de curve was not identical to that obtained using an acetone/1-propanol/toluene solvent system (Figure 1d) despite the fact that acetone is incorporated into the (S_a,S)-**1** crystal in both cases. This indicates that the diastereoselectivity of crystallization is not solely determined by the solvent permittivity but is also affected by the molecular structures of the solvents employed; similar observations have been made for other DCR systems.[9,12,13]

Crystallization was also carried out at room temperature in expectation of a temperature-dependent change in the aggregation state of amide **1** in solution. Interestingly, at room temperature, the threshold permittivity at which the deposited amide switched from (S_a,S)-**1**·solvent to (R_a,S)-**1** decreased as compared to that observed at −1 to −2 °C for each solvent system (Figure 1a−c). In contrast, the threshold permittivity for the reverse switching remained almost unchanged. With respect to the temperature-dependent change of the deposit diastereomers, Fuyuhiro et al. reported an interesting phenomenon during the enantiomeric resolution of (1*R*,3*S*,4*S*,7*R*)-3-bromocamphor-9-sulfonate (*d*-bcs$^-$) salts of racemic cobalt complex bis(ethylenediamine)oxalatocobalt(III) $[Co(ox)(en)_2]^+$. They found that the Δ-isomer precipitated as Δ-$[Co(ox)(en)_2]$(*d*-bcs) at 5 °C from an aqueous solution of the diastereomeric salts, whereas a pseudo racemic compound, Λ-$[Co(ox)(en)_2]$·Δ-$[Co(ox)(en)_2]$(*d*-bcs)$_2$·$2H_2O$, precipitated at 25 °C.[21]

X-ray Crystallographic Analyses of Amides (R_a,S)-1 and (S_a,S)-1. We successfully obtained single crystal X-ray

dx.doi.org/10.1021/jo3024285 | J. Org. Chem. 2013, 78, 597−605

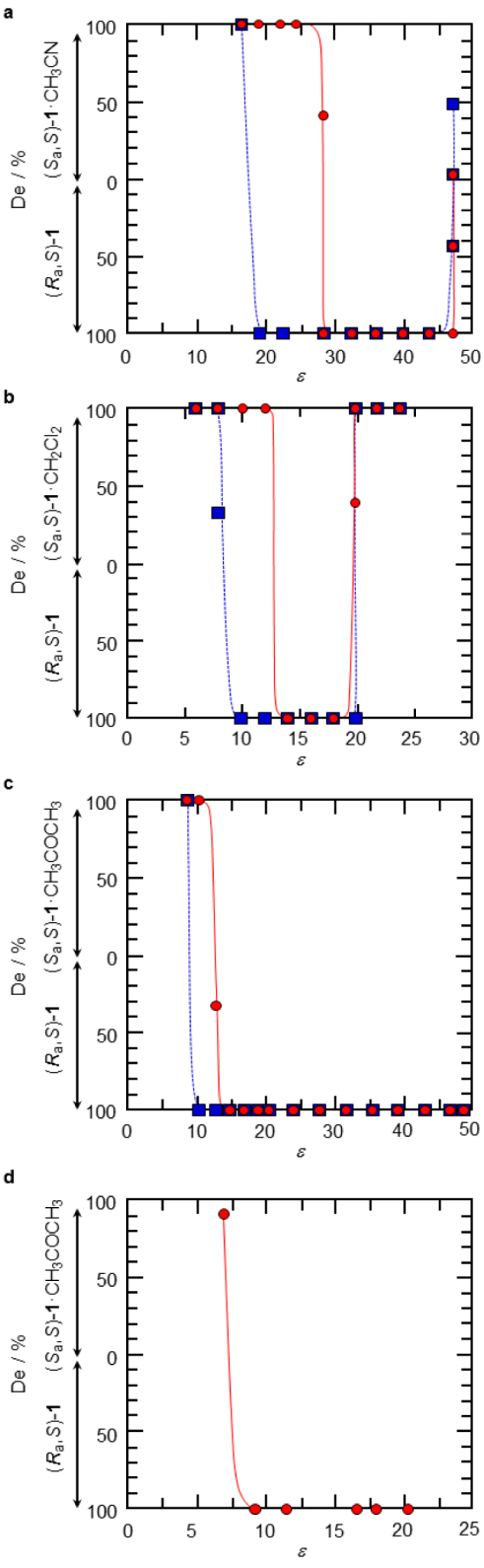

Figure 1. Dependence of the diastereomeric excess of deposited amide **1** on the permittivity of the crystallization solvent and the crystallization temperature: (a) acetonitrile/1-propanol/either hexane or water, (b) dichloromethane/2-propanol/either cyclohexane or water, (c) acetone/1-propanol/either hexane or water, and (d) acetone/1-propanol/toluene mixed solvents at −1 to −2 °C (red solid lines with ●) and 20 to 21.5 °C (blue broken lines with ■).

structures of (R_a,S)-**1**,[22] (S_a,S)-**1**·CH_3COCH_3,[22] (S_a,S)-**1**·CH_2Cl_2, and (S_a,S)-**1**·CH_3CN. The crystal data are summarized in Table 1. In all of the crystals, similar 2_1 helical structures are formed along one crystal axis by intramolecular hydrogen bonds between the carbamoyl NH and carboxy C═O groups and intermolecular hydrogen bonds between the carboxy OH and carbamoyl C═O groups (Figure 2a−d). In the crystal of (R_a,S)-**1**, the helices occur along the *b*-axis and are arranged parallel to each other along the *a*-axis, resulting in a layer with uneven top and bottom surfaces (Figure 3c). The layers, which are parallel to the *a*−*b* plane, pile up along the *c*-axis to match their bumps and hollows with those of the adjacent layers (Figure 3a and b); accordingly, a tight packing structure is achieved. The packing structures of the (S_a,S)-**1**·CH_3COCH_3 and (S_a,S)-**1**·CH_2Cl_2 crystals are quite similar. The crystal structure of (S_a,S)-**1**·CH_2Cl_2 is shown in Figure 4.[22] Similar to (R_a,S)-**1**, helices are created along the *b*-axis and gather together to form a layer parallel to the *a*−*b* plane (Figure 4c). One layer is rotated 180° around the *c*-axis and laid onto another layer to construct a laminated structure along the *c*-axis (Figure 4a and b). There are voids on the layer surfaces and they are filled with dichloromethane molecules (Figure 4c). In (S_a,S)-**1**·CH_3CN, two independent (S_a,S)-**1** molecules with slightly different conformations (Figure 2e) are connected alternately through intermolecular hydrogen bonds to form a 2_1 helix along the *c*-axis (Figure 2d). The helices gather together to form a layer parallel to the *a*−*c* plane (Figure 5c). Every adjacent layer is rotated 180° around both the *b*- and *c*-axes, and the layers pile up along the *b*-axis (Figure 5a and b). As in the case of (S_a,S)-**1**·CH_2Cl_2, there are voids on the layer surfaces that are filled with acetonitrile molecules (Figure 5c). As mentioned so far, the two diastereomeric amides form the same hydrogen-bond network in the crystals. The solvent molecules included into the (S_a,S)-**1** crystals do not participate in the network but rather simply fill the voids that originate from the molecular structure of the (S_a,S)-diastereomer. This is the first time that the DCR phenomenon was observed in a system that has an identical hydrogen-bond network in both diastereomeric crystals.

^{1}H NMR and IR Analysis of Amides (R_a,S)-1 and (S_a,S)-1. To elucidate the aggregation state of diastereomeric amides (R_a,S)-**1** and (S_a,S)-**1** in solution, ^{1}H NMR analysis was performed in mixed deuterated solvents of dichloromethane, 2-propanol, and either cyclohexane or water, with the solvent composition varied in the same manner as for the crystallization. Figure 6a and b shows the ε-dependent changes in the chemical shift values of the methyl groups of (S_a,S)-**1** and (R_a,S)-**1**, respectively, which were observed at −1 and 23 °C with a constant concentration (11.7 mM).[23] Each plot comprises three line segments with different slopes, the adjacent segments being connected by a node. The ε values (8.0 and 15.7) of the two nodes observed at 23 °C for (S_a,S)-**1** are almost the same as those of the corresponding nodes for (R_a,S)-**1** (7.8 and 16.0). In combination with the fact that the two amides feature the same hydrogen-bond network in the crystals (vide supra), these results suggest that their aggregation states are similar in the same solvents and that each node represents a transition between two different aggregation states. Each aggregate may exhibit different physical properties, such as solubility, and therefore exhibit different diastereoselectivity during crystallization. The ε values of the first nodes are in reasonable agreement with the ε value (8.1) at which the deposited diastereomer switched from (S_a,S)-**1**·CH_2Cl_2 to

dx.doi.org/10.1021/jo3024285 | J. Org. Chem. 2013, 78, 597−605

Table 1. X-ray Data for (R_a,S)-1, (S_a,S)-1·CH_3COCH_3, (S_a,S)-1·CH_2Cl_2, and (S_a,S)-1·CH_3CN

	(R_a,S)-**1**	(S_a,S)-**1**·CH_3COCH_3	(S_a,S)-**1**·CH_2Cl_2	(S_a,S)-**1**·CH_3CN
empirical formula	$C_{30}H_{23}NO_3$	$C_{33}H_{29}NO_4$	$C_{31}H_{25}Cl_2NO_3$	$C_{32}H_{26}N_2O_3$
formula weight	445.49	503.57	530.42	485.54
crystal system	monoclinic	orthorhombic	orthorhombic	monoclinic
space group	$P2_1$	$P2_12_12_1$	$P2_12_12_1$	$P2_1$
a (Å)	9.202(2)	11.325(2)	11.7329(12)	11.5356(2)
b (Å)	14.170(3)	13.892(2)	13.8113(15)	16.964(3)
c (Å)	9,299(2)	17.405(3)	16.8109(18)	13.756(2)
α (deg)	90.00	90.00	90.00	90.00
β (deg)	98.369(6)	90.00	90.00	96.314(2)
γ (deg)	90.00	90.00	90.00	90.00
V (Å^3)	1199.6(5)	2738.2(8)	2724.1(5)	2675.7(9)
Z	2	4	4	4
F(000)	468	1064	1104	1020
T (K)	100(2)	173(2)	223(2)	223(2)
ρ_{calc} (g cm^{-3})	1.233	1.222	1.293	1.205
reflections collected	8728	23258	15198	14571
independent reflections	5145	6381	6076	8117
R_{int}	0.0751	0.1004	0.0201	0.0304
μ (Mo Kα) (mm^{-1})	0.079	0.080	0.271	0.078
Data/restraints/parameters	5145/1/316	6381/0/355	6076/0/343	8117/1/687
R_1, wR_2 ($I > 2\sigma(I)$)	0.0577, 0.1276	0.0485, 0.1071	0.0527, 0.1425	0.0525, 0.1446
R_1, wR_2 (all data)	0.0723, 0.1333	0.0972, 0.1234	0.0620, 0.1527	0.0644, 0.1551
goodness-of-fit on F^2	0.928	0.984	1.040	1.077
largest diff. peak and hole (e Å^3)	0.254 and −0.235	0.156 and −0.193	0.632 and −0.679	0.374 and −0.238
intramolecular hydrogen bond: NH···O=C−OH (Å)	2.086	1.989	2.066	av. 2.053
intermolecular hydrogen bond: O=C−OH···O=C−NH (Å)	1.786	1.658	1.849	av. 1.609

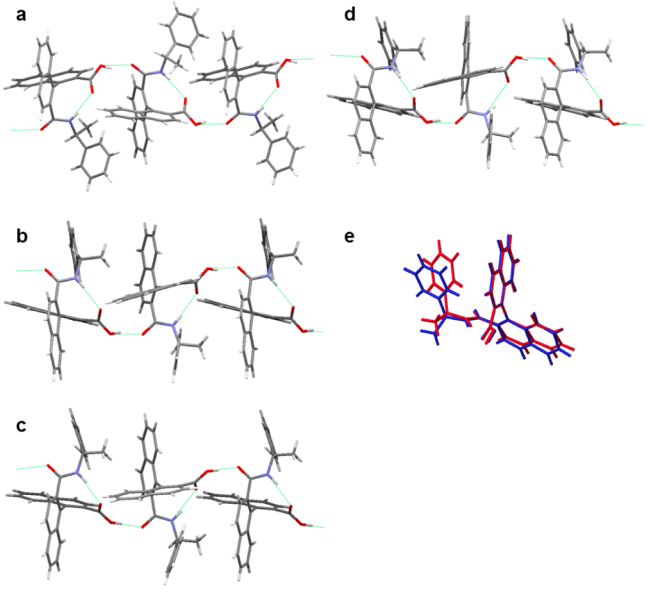

Figure 2. Hydrogen-bond network in (a) (R_a,S)-**1**, (b) (S_a,S)-**1**·CH_3COCH_3, (c) (S_a,S)-**1**·CH_2Cl_2, and (d) (S_a,S)-**1**·CH_3CN crystals. (e) Superimposition of two conformers of (S_a,S)-**1** in a unit cell of the (S_a,S)-**1**·CH_3CN crystal.

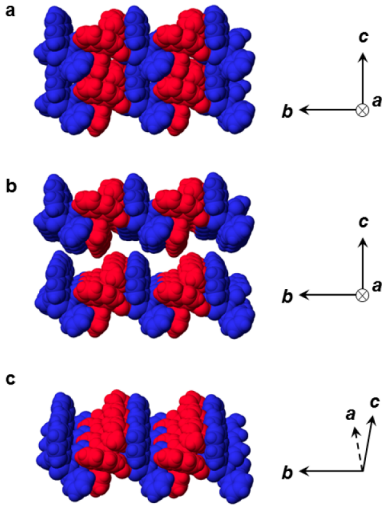

Figure 3. Crystal packing of (R_a,S)-**1**: (a) cross-section parallel to the b−c plane, (b) layers separated along the c-axis, and (c) surface of a separated layer.

(R_a,S)-**1** at room temperature (Figure 1b). However, the spectroscopy-determined ε values were hardly affected by the analytical temperature [8.2 for (S_a,S)-**1** and 7.8 for (R_a,S)-**1** at −1 °C versus 8.0 and 7.8, respectively, at 23 °C], whereas the deposited diastereomer switch shifted to a higher ε value (13.2) after lowering the crystallization temperature, as mentioned above. This discrepancy was attributed to the difference in solution concentration between the ^{1}H NMR and crystallization experiments. We then examined saturated amide solutions by ^{1}H NMR spectroscopy (Figure 6c and d).[23] Interestingly, the first nodes for both of the amides shifted to a significantly higher ε value at −1 °C [13.8 for (S_a,S)-**1** and 13.3 for (R_a,S)-**1**] but retained the same value at 23 °C. As a result, the ε values of the first nodes coincided with the ε values at which the deposited diastereomer changed from (S_a,S)-**1**·CH_2Cl_2 to (R_a,S)-**1** at both room temperature and −1 °C. This result supports the idea that the DCR phenomenon originates from an ε-dependent change in the aggregation state of the diastereomers. In contrast, the ε values of the second

dx.doi.org/10.1021/jo3024285 | J. Org. Chem. 2013, 78, 597−605

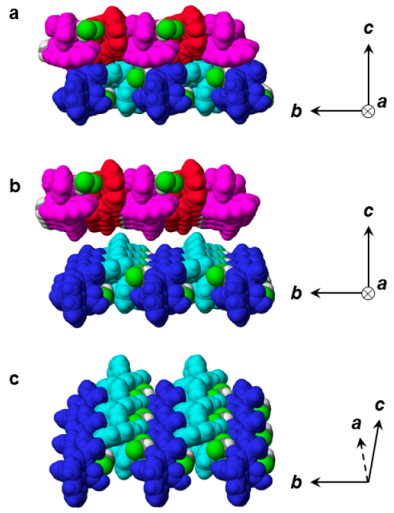

Figure 4. Crystal packing of (S_a,S)-**1**·CH_2Cl_2: (a) cross-section parallel to the b−c plane, (b) layers separated along the c-axis, and (c) surface of a separated layer.

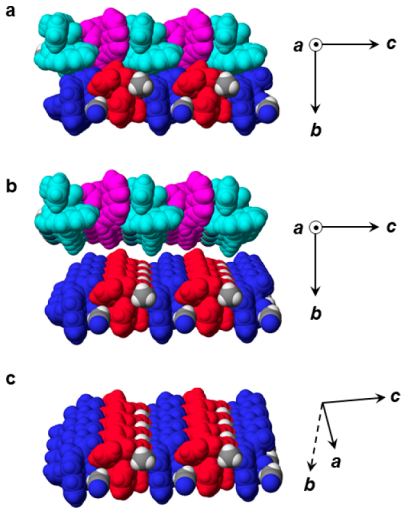

Figure 5. Crystal packing of (S_a,S)-**1**·CH_3CN: (a) cross-section parallel to the b−c plane, (b) layers separated along the b-axis, and (c) surface of a separated layer.

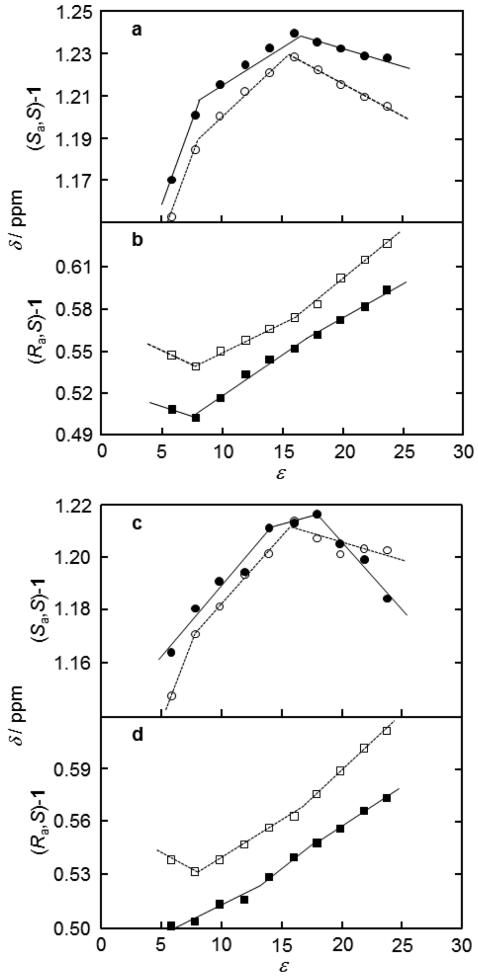

Figure 6. Changes in the chemical shift of the methyl protons of amides **1** depending on the solvent permittivity, concentration, and temperature: 11.7 mM solutions of (a) (S_a,S)-**1** and (b) (R_a,S)-**1** and saturated solutions of (c) (S_a,S)-**1** and (d) (R_a,S)-**1**. The solid lines with ● or ■ and broken lines with ○ or □ represent the chemical shifts at −1 and 23 °C, respectively. Solvent: dichloromethane-d_2/2-propanol-d_8/either cyclohexane-d_{12} or D_2O.

nodes (16.0−17.8) (Figure 6c and d) do not necessarily agree with the ε value at which the deposited diastereomer changed from (R_a,S)-**1** to (S_a,S)-**1**·CH_2Cl_2 (19.4) (Figure 1b). In addition, the former ε values depended on the temperature, whereas the latter did not. These observations imply that another factor also affects the diastereoselectivity of crystallization.

On the basis of the X-ray structures, it is reasonable to assume that amide **1** easily forms intramolecular hydrogen bonds between the carbamoyl NH and carboxy C═O groups and intermolecular hydrogen bonds between the carboxy OH and carbamoyl C═O groups in solution. Therefore, the wavenumbers of the carbamoyl and carboxy C═O stretching vibrations are good estimates of the extent of aggregation of the amide molecules. However, it is likely that the stretching vibrations are also affected by the intermolecular hydrogen bonds between the amide and alcohol molecules. Accordingly, IR analyses were performed using dichloromethane-based (75 vol %) mixed solvents containing different ratios of 1-propanol and hexane (total of 25 vol %) to moderate the effect of the alcohol. Figure 7 shows expanded IR spectra of the C═O stretching vibrations of amide **1** measured at room temperature. The wavenumber of the stretching vibration of the carbamoyl C═O group changed drastically near an ε of 7.6; the absorption appeared at 1615−1619 cm^{-1} and 1647−1656 cm^{-1} in solvents with lower and higher permittivity, respectively. Concurrently, the stretching vibration of the carboxy C═O group shifted to lower wavenumbers. These spectral changes can be interpreted as indicating that the amide molecules, which aggregate with the intermolecular hydrogen bonds in low-permittivity solvents, dissociate as the solvent permittivity increases; the reduced wavenumber of the carboxy C═O group suggests solvation of the carboxy group with alcohol molecules. When a 1:1 diastereomeric mixture of amide **1** was crystallized from mixed solvents of compositions similar to those employed for the IR analysis, a drastic change in the diastereomeric excess of the deposited amide was observed in the ε range of 8.9−11.1 (Figure S2 in Supporting Information), which is in reasonable agreement with the boundary of the spectral changes. These observations support that an ε-

dx.doi.org/10.1021/jo3024285 | J. Org. Chem. 2013, 78, 597−605

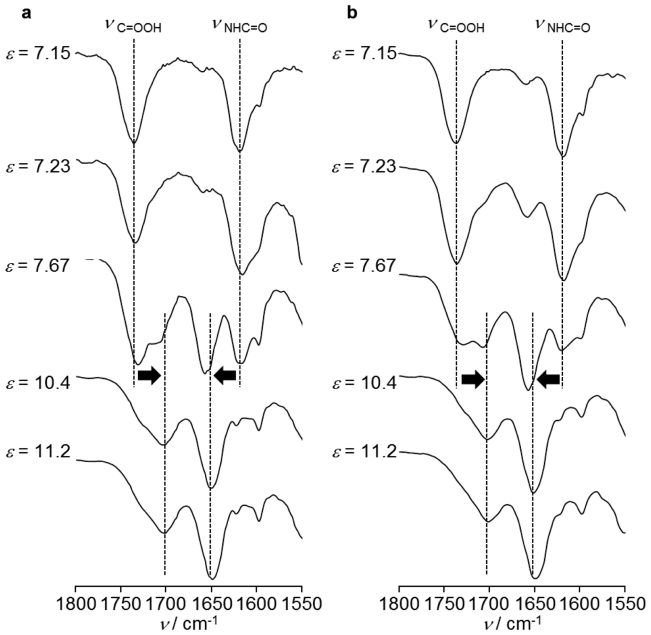

Figure 7. Change in the wavenumbers of the C=O stretching vibrations depending on the solvent permittivity for (a) (R_a,S)-**1** and (b) (S_a,S)-**1**. Concentration: 11.2 mM.

dependent change in the aggregation state causes the DCR phenomenon, at least in the lower ε range.

Absorption of Dichloromethane into Solvent-Free (S_a,S)-1 Crystals. As mentioned above, there is a minor but non-negligible difference in the ε values and their temperature dependence between the drastic change of the deposited diastereomer from (R_a,S)-**1** to (S_a,S)-**1**·CH_2Cl_2 during the crystallization (Figure 1b) and the second breakpoints of the chemical shift versus ε plots in the ^{1}H NMR analysis (Figure 6c and d), that is, the second transition point of the aggregation state of the amide. This suggests that another factor also influences the DCR phenomenon. As mentioned above, X-ray crystallographic analysis revealed that the only major difference between the crystal structures of (S_a,S)-**1** and (R_a,S)-**1** is the presence or absence of solvent molecules (Figures 3–5). In addition, in all of the DCR systems reported so far, one of the diastereomeric salts includes an additional species in the crystals.[7,9−14] This common feature led us to investigate the relationship between the permittivity of the crystallization solvents and the ease of incorporation of the solvent molecules into the crystals. Over the past decade, considerable attention has been focused on nanoporous molecular crystals and their absorption of guest molecules.[24] Unlike metal−organic frameworks (MOFs), covalent organic frameworks (COFs), and network polymers, nanoporous molecular crystals do not have extended network structures formed by coordination or covalent bonds, but rather, they are composed of discrete organic molecules with weak noncovalent interactions. In addition, some nanoporous molecular crystals have disconnected voids to absorb guest molecules rather than interconnected pore channels. For example, Atwood and coworkers reported that crystals of *p*-*tert*-butylcalix[4]arene, which do not have interconnected pore channels, absorbed small molecules from a gas or liquid phase into its molecular cavity; this is accompanied by a phase transition that results in inclusion crystals having a different crystal lattice than the original crystals.[25,26] We envisaged the use of such a phenomenon, i.e., the inclusion of guest molecules into host crystals, to examine the effect of solvent permittivity on the ease of incorporation of solvent molecules into crystals.

Solvent-free (S_a,S)-**1** crystals were prepared by heating (S_a,S)-**1**·CH_2Cl_2 at 120 °C in vacuo (0.5−1.0 kPa) for 24 h. Powder X-ray diffraction (PXRD) analyses of the solvent-free (S_a,S)-**1** and (S_a,S)-**1**·CH_2Cl_2 revealed that they had different crystal lattices (Figure S3 in Supporting Information). The solvent-free crystals were then immersed in a mixed solvent comprising hexane, acetylacetone, and dichloromethane at a volumetric ratio of 5.5:4.5:0.5 (ε = 15.1) at −1 to −2 °C for 10 h.[27] The resulting crystals were collected by filtration, dried in vacuo, and analyzed by ^{1}H NMR spectroscopy. It was revealed that they contained dichloromethane; the average number of dichloromethane molecules included in the crystals per (S_a,S)-**1** molecule (n_{av}) was 0.8. The PXRD pattern of the dichloromethane-containing crystals was in reasonable agreement with that of (S_a,S)-**1**·CH_2Cl_2 (Figure S3 in Supporting Information). These observations clearly indicate that the solvent-free (S_a,S)-**1** crystals absorb dichloromethane and convert into (S_a,S)-**1**·CH_2Cl_2. The ε-dependence of the inclusion ratio, n_{av}, was then examined at two different temperatures (Figure 8).

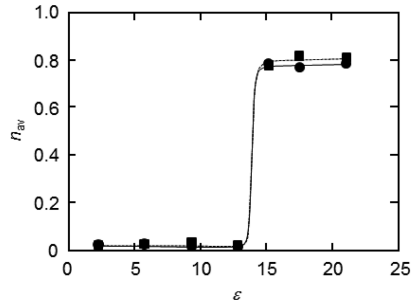

Figure 8. Dependence of the inclusion ratio of dichloromethane to (S_a,S)-**1** on the solvent permittivity and temperature for the absorption of dichloromethane into solvent-free (S_a,S)-**1** crystals: measurements at −1 to −2 °C (solid line with ●) and 22 to 23 °C (broken line with ■). Solvent: dichloromethane/acetylacetone/hexane.

Although the solvent-free crystals absorbed hardly any dichloromethane from mixed solvents with ε values of 12.8 or less, higher-permittivity solvents gave inclusion crystals with almost constant n_{av} values (~0.8); this clearly indicates that in high-permittivity solvents the low-polarity dichloromethane molecules are easily incorporated into the crystals. The temperature did not affect the threshold permittivity, as in the case of the drastic change of the deposited diastereomer from (R_a,S)-**1** to (S_a,S)-**1**·CH_2Cl_2 during crystallization (Figure 1b). However, these threshold ε values do not necessarily agree well with each other. This is attributable to the fact that they represent different phenomena: in the former, the solvent molecules are incorporated into the crystals, whereas in the latter, the solvent molecules construct crystals with the amide molecules. Considering this fundamental difference, it may be concluded that in high-permittivity solvents, the diastereomer deposited is affected by the ε-dependent change in the ease of incorporation of the solvent molecules into the crystals.

Mechanistic Consideration. On the basis of these observations, a feasible molecular mechanism for the present DCR phenomenon is proposed (Figure 9). In a low-permittivity solvent (Figure 9a), the amide molecules strongly associate with each other via intermolecular hydrogen bonds.

dx.doi.org/10.1021/jo3024285 | J. Org. Chem. 2013, 78, 597−605

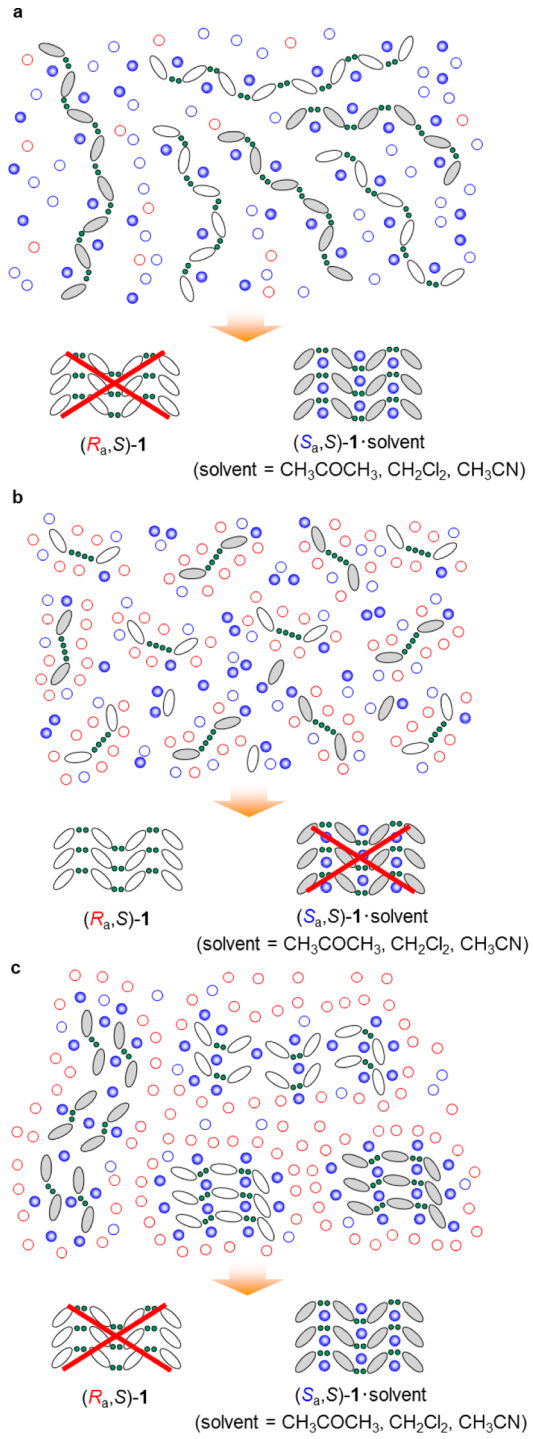

Figure 9. Feasible molecular mechanism for the diastereoselective crystallization of (R_a,S)-**1** or (S_a,S)-**1**·solvent from solvents with (a) low, (b) intermediate, and (c) high ε values. The white and gray ellipsoids represent the (R_a,S)-**1** and (S_a,S)-**1** molecules, respectively. The blue spheres represent solvent molecules that can be incorporated into (S_a,S)-**1**·solvent. The blue and red circles represent other solvent molecules with lower and higher ε values, respectively. The dotted lines indicate intermolecular hydrogen bonds.

Acetone, dichloromethane, and acetonitrile molecules, which can be incorporated into (S_a,S)-**1**·solvent crystals as space fillers, have relatively high polarity and, therefore, prefer incorporation into the hydrophilic part of the amide aggregate to diffusion into the mixed solvent with low polarity. This solvation with space-filling molecules is favorable for the crystallization of (S_a,S)-**1**·solvent because its components preorganize in solution. In contrast, the aggregate of (R_a,S)-**1** requires desolvation to form crystals. Consequently, (S_a,S)-**1**·solvent will preferentially crystallize from low-permittivity solvents. As the solvent permittivity increases, the high-polarity component of the mixed solvent solvates the amide molecules, resulting in dissociation of the amide aggregate (Figure 9b). The space-filling molecules, which are similar in polarity to the mixed solvent, diffuse into solution. Under these conditions, (R_a,S)-**1** should preferentially crystallize because the (R_a,S)-**1** crystal has an advantage over (S_a,S)-**1**·solvent with regard to the entropy loss associated with crystallization. Further, it is apparently easier for the amide aggregate to dissociate at higher temperatures. This would be the reason that the threshold permittivity at which the deposited amide switched from (S_a,S)-**1**·solvent to (R_a,S)-**1** decreased with increasing crystallization temperature (vide supra). In a high-permittivity solvent (Figure 9c), the amide molecules associate via hydrophobic interactions to form aggregates, which are preferable to the high-permittivity solvent for the space-filling molecules owing to the polarity similarities. As a result, the space-filling molecules are readily included into the aggregates. Under these conditions, the crystallization of (S_a,S)-**1**·solvent is promoted by preorganization.

CONCLUSION

In conclusion, we succeeded in applying DCR to the separation of a pair of diastereomeric amides, (RS_a,S)-**1**. Since the crystal structures of the two diastereomers are very similar and there is no complex equilibration in solution, such as dissociation equilibration of diastereomeric salts, this is the simplest system of the hitherto reported applications of DCR. As a result, we were able to elucidate a feasible molecular mechanism from two different ε-dependent changes, i.e., a change in the aggregation state of the amide molecules and a change in ease of incorporation of solvent molecules into the crystals; it is not necessary for the diastereomers to have different aggregation states or ε-dependent changes. We expect that the findings in this study will contribute to clarifying the mechanisms for more complex diastereomeric salt-based DCR systems.

EXPERIMENTAL SECTION

General. ^{1}H NMR spectra were measured with tetramethylsilane as an internal standard. IR spectra were recorded using a liquid cell (0.1 mm thick) with NaCl windows. Amide (RS_a,S)-**1** was prepared according to the literature procedure.[19] Solvents for the crystallization, IR analysis, and absorption experiment were distilled before use except for alcohols. Other materials were used as purchased.

Typical Procedure for the Crystallization of Amide (RS_a,S)-1. To a 1:1 diastereomeric mixture of amide (RS_a,S)-**1** (165 mg, 0.370 mmol) in a 30 mL screw-cap vial was added portionwise a mixed solvent composed of hexane, 1-propanol, and acetone at a volumetric ratio of 2:5:1 (ε = 8.9) at 40−50 °C until a homogeneous solution was formed (13 mL). The solution was gradually cooled to −2 °C over a period of 6.5 h and left at the temperature for 3 d to induce crystallization. The crystals were collected by filtration, washed with the mixed solvent (5.0 mL), and dried in vacuo (0.5−1.0 kPa) at room temperature to give inclusion crystal (S_a,S)-**1**·acetone (43.2 mg, 23%). The ^{1}H NMR analysis of amide **1** in $CDCl_3$ differentiates well the methyl signals of (R_a,S)-isomer (0.90 ppm) and (S_a,S)-isomer (1.41 ppm). By making use of this fact, the diastereomeric excess of the sample was determined to 100% de.

Single Crystal X-ray Diffraction Studies. Single crystals of (R_a,S)-**1**, (S_a,S)-**1**·CH_2Cl_2, and (S_a,S)-**1**·CH_3CN were obtained by

dx.doi.org/10.1021/jo3024285 | J. Org. Chem. 2013, 78, 597−605

crystallizing the corresponding diastereomerically pure amides from acetonitrile [(R_a,S)-**1** and (S_a,S)-**1**·CH_3CN] or dichloromethane [(S_a,S)-**1**·CH_2Cl_2]. Single crystals of (S_a,S)-**1**·CH_3COCH_3 were obtained by vapor diffusion of hexane into a solution of (S_a,S)-**1** in acetone at room temperature. Single-crystal X-ray diffraction data were collected with a CCD diffractometer using Mo Kα radiation (λ = 0.71073 Å). Data integration and reduction were performed with SAINT and XPREP software and the absorption correction was performed by the semiempirical method with SADABS.[28] The structure was solved by direct method using SHELXS-97 and refined by using least-squares method on F^2 with SHELXL-97.[29] X-ray analysis was undertaken using Yadokari-XG 2009.[30] Crystal data and measurement details are summarized in Table 1.

Typical Procedure for the Absorption of Dichloromethane into Solvent-Free (S_a,S)-1 Crystals. Solvent-free (S_a,S)-**1** crystals (40.0 mg, 89.8 μmol), which were prepared by heating inclusion crystal (S_a,S)-**1**·CH_2Cl_2 at 120 °C in vacuo (0.5−1.0 kPa) for 24 h, were immersed in a mixed solvent (1.0 mL) composed of hexane, acetylacetone,[27] and dichloromethane at a volumetric ratio of 5.5:4.5:0.5 (ε = 15.1) at −1 to −2 °C. After 10 h, the resulting crystals were collected by filtration, washed with the mixed solvent (5 mL), and dried in vacuo (0.5−1.0 kPa) at room temperature to give inclusion crystal (S_a,S)-**1**·CH_2Cl_2 (33.6 mg), the n_{av} value of which was determined to be 0.8 by ^{1}H NMR analysis.

■ ASSOCIATED CONTENT

Supporting Information

CIF files for (R_a,S)-**1**, (S_a,S)-**1**·CH_3COCH_3, (S_a,S)-**1**·CH_2Cl_2, and (S_a,S)-**1**·CH_3CN; crystallization data for Figure 1; changes in the chemical shift of the methine protons of amides **1** depending on the solvent permittivity, concentration, and temperature; dependence of the diastereomeric excess of deposited amide **1** on the permittivity of the mixed solvent employed for the IR analysis; and PXRD data for the crystals of (S_a,S)-**1**. This material is available free of charge via the Internet at http://pubs.acs.org.

■ AUTHOR INFORMATION

Corresponding Author

*E-mail: hattori@orgsynth.che.tohoku.ac.jp.

Notes

The authors declare no competing financial interest.

■ ACKNOWLEDGMENTS

This study was supported in part by a grant-in-aid from Tohoku University International Advanced Research and Education Organization. T.H. wishes to thank Toray Fine Chemicals Co., Ltd. for financial support.

■ REFERENCES

(1) (a) Jacques, J.; Collet, A.; Wilen, S. H. *Enantiomers, Racemates, and Resolutions*; Wiley: New York, 1981. (b) Kozma, D. *CRC Handbook of Optical Resolution via Diastereomeric Salt Formation*; CRC: Boca Raton, 2002.

(2) Rouhi, A. M. *Chem. Eng. News* **2003**, No. May 5, 45.

(3) (a) Dyer, U. C.; Henderson, D. A.; Mitchell, M. B. *Org. Process Res. Dev.* **1999**, *3*, 161. (b) Borghese, A.; Libert, V.; Zhang, T.; Alt, C. A. *Org. Process Res. Dev.* **2004**, *8*, 532.

(4) (a) Vries, T.; Wynberg, H.; van Echten, E.; Koek, J.; ten Hoeve, W.; Kellogg, R. M.; Broxterman, Q. B.; Minnaard, A.; Kaptein, B.; van der Sluis, S.; Hulshof, L.; Kooistra, J. *Angew. Chem.* **1998**, *110*, 2491; *Angew. Chem., Int. Ed.* **1998**, *37*, 2349. (b) Kellogg, R. M.; Kaptein, B.; Vries, T. R. *Top. Curr. Chem.* **2007**, *269*, 159.

(5) (a) Brands, K. M. J.; Davies, A. J. *Chem. Rev.* **2006**, *106*, 2711. (b) Anderson, N. G. *Org. Process Res. Dev.* **2005**, *9*, 800. (c) Yoshioka, R. *Top. Curr. Chem.* **2007**, *269*, 83.

(6) Review: Sakai, K.; Sakurai, R.; Nohira, H. *Top. Curr. Chem.* **2007**, *269*, 199.

(7) Sakai, K.; Sakurai, R.; Hirayama, H. *Tetrahedron: Asymmetry* **2004**, *15*, 1073.

(8) Pasteur, L. *C. R. Hebd. Seances Acad. Sci.* **1853**, *37*, 162.

(9) Sakai, K.; Sakurai, R.; Nohira, H.; Tanaka, R.; Hirayama, N. *Tetrahedron: Asymmetry* **2004**, *15*, 3495.

(10) Sakai, K.; Sakurai, R.; Hirayama, N. *Tetrahedron: Asymmetry* **2006**, *17*, 1812.

(11) Sakurai, R.; Yuzawa, A.; Sakai, K.; Hirayama, N. *Cryst. Growth Des.* **2006**, *6*, 1606.

(12) Taniguchi, K.; Aruga, M.; Yasutake, M.; Hirose, T. *Org. Biomol. Chem.* **2008**, *6*, 458.

(13) Hirose, T.; Begum, M.; Islam, M. S.; Taniguchi, K.; Yasutake, M. *Tetrahedron: Asymmetry* **2008**, *19*, 1641.

(14) Sakurai, R.; Sakai, K.; Kodama, K.; Yamaura, M. *Tetrahedron: Asymmetry* **2012**, *23*, 221.

(15) Review: Sakai, K.; Sakurai, R.; Hirayama, N. *Top. Curr. Chem.* **2007**, *269*, 233.

(16) Sakai, K.; Sakurai, R.; Akimoto, T.; Nohira, H. *Org. Biomol. Chem.* **2005**, *3*, 360.

(17) Taniguchi, K.; Sakurai, R.; Sakai, K.; Yasutake, M.; Hirose, T. *Bull. Chem. Soc. Jpn.* **2006**, *79*, 1084.

(18) Kato, Y.; Kitamoto, Y.; Morohashi, N.; Kuruma, Y.; Oi, S.; Sakai, K.; Hattori, T. *Tetrahedron Lett.* **2009**, *50*, 1998.

(19) Oi, S.; Matsuzaka, Y.; Yamashita, J.; Miyano, S. *Bull. Chem. Soc. Jpn.* **1989**, *62*, 956.

(20) The values of dielectric constants of mixed solvents were calculated as the weighted average of dielectric constants of components. See ref 9.

(21) Fuyuhiro, A.; Yamanari, K.; Shimura, Y. *Bull. Chem. Soc. Jpn.* **1979**, *52*, 1420.

(22) For the crystal structure of (S_a,S)-**1**·CH_3COCH_3, see ref 18.

(23) Similar ε-dependent changes were observed for the methine protons of (S_a,S)-**1** and (R_a,S)-**1** (Figure S1 in Supporting Information).

(24) Reviews: (a) Holst, J. R.; Trewin, A.; Cooper, A. I. *Nat. Chem.* **2010**, *2*, 915. (b) McKeown, N. B. *J. Mater. Chem.* **2010**, *20*, 10588. (c) Tian, J.; Thallapally, P. K.; McGrail, B. P. *CrystEngComm* **2012**, *14*, 1909.

(25) (a) Atwood, J. L.; Barbour, L. J.; Jerga, A.; Schottel, B. L. *Science* **2002**, *298*, 1000. (b) Atwood, J. L.; Barbour, L. L.; Jerga, A. *Angew. Chem., Int. Ed.* **2004**, *43*, 2948. (c) Thallapally, P. K.; McGrail, B. P.; Dalgarno, S. J.; Schaef, H. T.; Tian, J.; Atwood, J. L. *Nat. Mater.* **2008**, *7*, 146.

(26) See also: (a) Gorbatchuk, V. V.; Tsifarkin, A. G.; Antipin, I. S.; Solomonov, B. N.; Konovalov, A. I.; Seidel, J.; Baitalov, F. *J. Chem. Soc., Perkin Trans. 2* **2000**, 2287. (b) Gorbatchuk, V. V.; Tsifarkin, A. G.; Antipin, I. S.; Solomonov, B. N.; Konovalov, A. I.; Lhotak, P.; Stibor, I. *J. Phys. Chem. B* **2002**, *106*, 5845. (c) Enright, G. D.; Udachin, K. A.; Moudrakovski, I. L.; Ripmeester, J. A. *J. Am. Chem. Soc.* **2003**, *125*, 9896. (d) Ziganshin, M. A.; Yakimov, A. V.; Safina, G. D.; Solovieva, S. E.; Antipin, I. S.; Gorbatchuk, V. V. *Org. Biomol. Chem.* **2007**, *5*, 1472. (e) Brouwer, D. H.; Moudrakovski, I. L.; Udachin, K. A.; Enright, G. D.; Ripmeester, J. A. *Cryst. Growth Des.* **2008**, *8*, 1878. (f) Udachin, K. A.; Moudrakovski, I. L.; Enright, G. D.; Ratcliffe, C. I.; Ripmeester, J. A. *Phys. Chem. Chem. Phys.* **2008**, *10*, 4636. (g) Morohashi, N.; Noji, S.; Nakayama, H.; Kudo, Y.; Tanaka, S.; Kabuto, C.; Hattori, T. *Org. Lett.* **2011**, *13*, 3292. (h) Morohashi, N.; Shibata, O.; Hattori, T. *Chem. Lett.* **2012**, *41*, 1412.

(27) The solvent-free crystals absorbed 1-propanol and 2-propanol, and therefore, acetylacetone was employed as a high-permittivity solvent in this experiment.

(28) (a) *SMART, SAINT, and XPREP, Area Detector Control and Data Integration and Reduction Software*; Bruker Analytical Xray Instruments Inc.: Madison, WI, 1995. (b) Sheldrick, G. M. *SADABS, Empirical Absorption Correction Program for Area Detector Data*; University of Göttingen: Göttingen, Germany, 1996.

(29) Sheldrick, G. M. *SHELX-97, Programs for the Refinement of Crystal structures*; University of Göttingen: Göttingen, Germany, 1997.
(30) (a) Wakita, K. *Yadokari-XG, Software for Crystal Structure Analyses*, 2001. (b) Kabuto, C.; Akine, S.; Nemoto, T.; Kwon, E. *J. Cryst. Soc. Jpn.* **2009**, *51*, 218.